Effective Boundary Conditions for the Laplace Equation with a Rough Boundary

Kausik Sarkar; Andrea Prosperetti

Proceedings: Mathematical and Physical Sciences, Vol. 451, No. 1942 (Nov. 8, 1995), 425-452.

Stable URL:
http://links.jstor.org/sici?sici=0962-8444%2819951108%29451%3A1942%3C425%3AEBCFTL%3E2.0.CO%3B2-E

Proceedings: Mathematical and Physical Sciences is currently published by The Royal Society.

Your use of the JSTOR archive indicates your acceptance of JSTOR's Terms and Conditions of Use, available at http://www.jstor.org/about/terms.html. JSTOR's Terms and Conditions of Use provides, in part, that unless you have obtained prior permission, you may not download an entire issue of a journal or multiple copies of articles, and you may use content in the JSTOR archive only for your personal, non-commercial use.

Please contact the publisher regarding any further use of this work. Publisher contact information may be obtained at http://www.jstor.org/journals/rsl.html.

Each copy of any part of a JSTOR transmission must contain the same copyright notice that appears on the screen or printed page of such transmission.

JSTOR is an independent not-for-profit organization dedicated to creating and preserving a digital archive of scholarly journals. For more information regarding JSTOR, please contact support@jstor.org.

http://www.jstor.org/
Wed Dec 1 11:51:22 2004

Effective boundary conditions for the Laplace equation with a rough boundary

By Kausik Sarkar and Andrea Prosperetti

Department of Mechanical Engineering, The Johns Hopkins University, Baltimore, MD 21218, USA

The problem of replacing Dirichlet or Neumann conditions on a stochastically embossed surface by approximate effective conditions on a smooth surface is studied for potential fields satisfying the Laplace equation. A combination of ensemble averaging and multiple-scattering techniques is used. It is shown that for the Dirichlet case the effective boundary condition becomes mixed and establishes a relation between the averaged field and its normal derivative. For the Neumann problem the normal derivative on the smooth surface equals a suitable combination of first- and second-order derivatives tangent to the surface. Explicit results are given for small boss concentration and illustrated with the examples of spheroidal and spherical bosses. For the Dirichlet case with hemispherical bosses, direct numerical-simulation results are presented up to area coverages of 75%. An application of the results to the calculation of the added mass of a rough sphere in potential flow, of the capacitance of a rough spherical conductor, and of the transmission and reflection of long water waves at a smooth–rough bottom transition aids in their physical interpretation.

1. Introduction

A considerable amount of work has been devoted to the problem of wave scattering from rough surfaces (Biot 1968; Tolstoy 1980, 1984, 1986; Ogilvy 1987, 1991; Twersky 1957, 1983; Lucas & Twersky 1988). The objective pursued in these studies is that of substituting the exact boundary conditions that hold on the rough surface by simpler, if approximate, conditions applied on a smooth approximation to it. Typically this research has employed methods and techniques developed in the context of multiple-scattering theory (see, for example, Foldy 1945).

The literature devoted to the corresponding problem in connection with other equations seems however to be rather sparse. The propagation of water waves in a shallow channel with a rough bottom has led Rosales & Papanicolaou (1983) to study the Laplace equation in the presence of a Neumann boundary condition on a rough surface. Miksis & Davis (1994) have studied the advancing of a gas–liquid contact line over a rough surface. Beavers & Joseph (1967) and many others (Saffman 1971; Taylor 1971; Richardson 1971; Nield 1983; Jansons 1988) have considered the related problem of the effective boundary conditions at the surface separating a porous medium from clear fluid.

In this paper we develop a method that appears to be of broad applicability to a variety of problems. The method is presented here for the case of the Laplace

Proc. R. Soc. Lond. A (1995) **451**, 425–452
© 1995 The Royal Society
Printed in Great Britain

TEX Paper

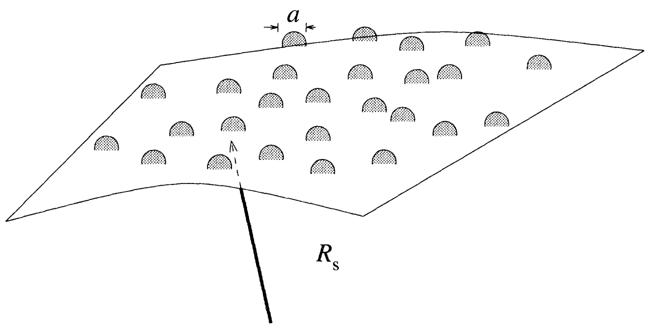

Figure 1. Model of an embossed surface.

equation. A companion paper (Sarkar & Prosperetti 1996) deals with Stokes flow. The Helmholtz problem is addressed in Sarkar (1994).

The rough surface that we envisage here is of the type introduced by Twersky (1951) and studied extensively by him and other writers (see, for example, the review by Ogilvy (1987) and references therein). It consists of small irregularities—bosses—placed on an underlying smooth surface (figure 1), and is therefore different from other rough-surface models in which the roughness may be characterized as being of the 'wavy' type. It is this circumstance that enables us to develop an approach to the problem inspired by multiple-scattering theory. We calculate the effective boundary conditions to be applied to the field $\langle \phi \rangle$ by taking the ensemble average of the exact field ϕ over all possible arrangements of the bosses on the smooth surface. As in all similar analyses, we encounter a closure problem that, in the dilute limit, is dealt with in the way introduced by Foldy (1945). For the particular case of hemispherical bosses at finite concentrations we resolve the closure issue by direct numerical simulation (§ 8).

With suitable assumptions as to the smallness of the irregularities, for homogeneous Dirichlet conditions on the exact rough surface, we find a mixed effective boundary condition on the approximating smooth surface establishing the proportionality of the field to its normal gradient. For the Neumann case and a uniform distribution of bosses, the normal gradient is found to be proportional to the tangential Laplacian of the field. In the presence of surface gradients of the boss concentration, a further term appears. To illustrate the physical meaning of these results, in § 10 we briefly consider applications to the calculation of the added mass of a rough sphere in potential flow, of the electrical capacitance of a conductor in the shape of a rough sphere, and to the transmission and reflection of surface waves in a shallow channel, the bottom of which changes from smooth to rough.

In § 2 we present the mathematical formulation of the problem and in § 3 and 4 develop the necessary statistical tools. In § 5 an exact general non-local form of the boundary condition is derived for the Dirichlet and Neumann problems. Explicit dilute-limit results are obtained in § 6 and illustrated for bosses of several different shapes in § 7. The two-dimensional case is briefly considered in § 9.

In some of the simpler cases (e.g. hemispherical bosses) the dilute-limit results that we find can be recovered from the multiple-scattering literature simply by setting the wavenumber to zero (see, for example, Biot 1968; Tolstoy 1980, 1984, 1986; Ogilvy 1987, 1991; Twersky 1957). However, the Helmholtz operator presents difficulties that do not arise with the Laplace operator, such as a more limited set of separable coordinate systems and the presence of the wavelength as an additional

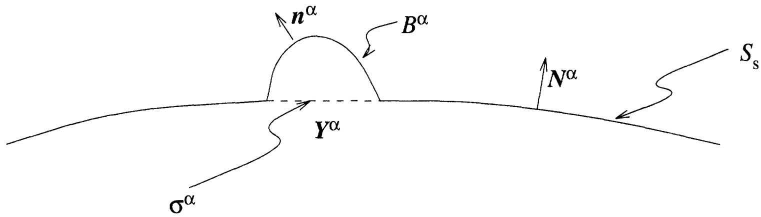

Figure 2. Definition of quantities pertaining to an individual boss.

length scale. As a consequence, on the one hand our results can be derived in a more straightforward way than the corresponding multiple-scattering results and, on the other, we are able to solve problems that have not been solved for the Helmholtz equation. In particular, the analogue of our direct numerical simulations cannot be found in the multiple-scattering literature. Furthermore, for plane surfaces, we are able to obtain an exact result that can form the basis for further extension of the theory by both analytical and numerical means. Examples are higher order terms in the boss concentration or in the ratio of the boss to the body scale. It would be very difficult to pursue such developments on the basis of the available results for the Helmholtz operator.

2. Formulation

We consider the Laplace equation for a field ϕ

$$\nabla^2 \phi = 0 \tag{1}$$

in a domain Ω bounded (possibly only in part) by a 'rough' boundary $\partial\Omega_r$. The remaining part $\partial\Omega_s$ of the boundary, if any, is assumed to be smooth and far away from $\partial\Omega_r$ in a sense to be made more precise below.

We only wish to consider boundaries that would be smooth except for the presence of non-overlapping bosses, or 'bumps', placed over a smooth surface S_s. Thus, we exclude roughnesses that might loosely be described as being of a 'wavy' type. More precisely, we shall think of $\partial\Omega_r$ as constructed as follows (figure 1). Start from a smooth surface S_s with a minimum radius of curvature R_s, and consider an open surface B of such a shape that it can be closed by the addition of the portion of a plane, the 'base'. We assume that B is small in the sense that its dimensions, of order a, are much smaller than R_s. The rough boundary $\partial\Omega_r$ is generated by placing identical copies of B over S_s. This construction is immediately generalizable to bosses of different shapes and sizes and to the corresponding two-dimensional problem in which the bosses are infinitely long ridges (see § 9).

According to this construction, $\partial\Omega_r$ consists of the surfaces B^α, $\alpha = 1, 2, \ldots, N$ of the N bosses, and of the portion of S_s not covered by them. We shall denote by σ^α the base of the αth boss, i.e. its intersection with S_s (figure 2). Note that $B^\alpha \bigcup \sigma^\alpha$ constitutes a closed surface. The boundary $\partial\Omega_r$ coincides with S_s away from the bases σ^α and it has therefore a slowly varying normal in these regions.

On $\partial\Omega_r$, ϕ is subject to homogeneous Dirichlet

$$\phi = 0 \tag{2}$$

or Neumann

$$\boldsymbol{n} \cdot \nabla\phi = 0 \tag{3}$$

boundary conditions. The solution of the problem is made unique by stipulating suitable boundary conditions—that need not be specified—on the remaining part of the boundary $\partial\Omega_s$. Our objective is to replace the Dirichlet or Neumann conditions on the rough surface $\partial\Omega_r$ by approximate boundary conditions on the smooth surface S_s.

We represent the solution ϕ in the form

$$\phi = \phi_0 + \sum_{\alpha=1}^{N} \chi^\alpha. \tag{4}$$

Loosely speaking, this decomposition may be interpreted by saying that ϕ_0 is the zeroth-order approximation to the solution of the problem obtained by substituting the actual rough boundary with its smooth approximation S_s, while each χ^α accounts for the effect of the αth irregularity. More precisely, we make the decomposition (4) well-defined by stipulating that ϕ_0 satisfies either the Dirichlet

$$\phi_0 = 0 \tag{5}$$

or Neumann

$$\boldsymbol{N} \cdot \nabla\phi_0 = 0 \tag{6}$$

conditions on S_s, and the prescribed boundary conditions on the smooth boundary $\partial\Omega_s$. Here $\boldsymbol{N}$ is the local unit normal to S_s directed into Ω (figure 2). Each χ^α also satisfies the Laplace equation and vanishes on the regular part of the boundary $\partial\Omega_s$ that is taken to lie effectively at infinity on the scale a of the bosses. Furthermore, on $S_s - \sigma^\alpha$,

$$\chi^\alpha = 0 \quad \text{or} \quad \boldsymbol{N} \cdot \nabla\chi^\alpha = 0, \tag{7}$$

while, on the αth boss, the relations arising from the complete Dirichlet (2) or Neumann (3) conditions are satisfied. To express these conditions it is convenient to define

$$\psi^\alpha = \phi_0 + \sum_{\beta\neq\alpha} \chi^\beta, \tag{8}$$

so that, for every $\alpha = 1, 2, \ldots, N$,

$$\phi = \chi^\alpha + \psi^\alpha. \tag{9}$$

On B^α then χ^α satisfies

$$\chi^\alpha = -\psi^\alpha \tag{10}$$

or

$$\boldsymbol{n}^\alpha \cdot \nabla\chi^\alpha = -\boldsymbol{n}^\alpha \cdot \nabla\psi^\alpha, \tag{11}$$

where $\boldsymbol{n}^\alpha$ is the normal to B^α directed into Ω. It should be explicitly noted that each χ^α is well defined also inside the other bosses and satisfies either one of (7) on their bases. Inside the boss α we define χ^α to be zero. This definition makes the expression (4) well defined everywhere in the domain bounded by the smooth surface S_s.

In the literature on multiple scattering the fields χ^α and ψ^α are referred to as the 'scattered' and 'incident' fields, respectively.

3. Probabilistic framework

Although in some cases the exact solution of the previous problem can be obtained numerically up to a very large number of surface irregularities, for many applications it is neither useful nor desirable to deal with such a vast amount of information. In these situations, suitable average quantities are of greater practical interest and it is the calculation of such quantities that is our concern here.

We make use of the method of ensemble averaging and consider a large number of rough surfaces, all obtained from S_s by different arrangements of the N bosses. Each arrangement is termed a *configuration* and denoted by $\mathcal{C}^{\mathrm{N}} \equiv (\boldsymbol{Y}^1, \boldsymbol{Y}^2, \ldots, \boldsymbol{Y}^{\mathrm{N}})$, where $\boldsymbol{Y}^\alpha$ is the position of a reference point of σ^α (e.g. the centre of symmetry) referred to an arbitrary system of curvilinear coordinates on S_s. A particular configuration occurs in the ensemble with a probability proportional to $P(\mathcal{C}^{\mathrm{N}}) \equiv P(N)$. Since the irregularities are indistinguishable, it is convenient to use the normalization (see, for example, Batchelor 1972)

$$N! = \int \mathrm{d}\mathcal{C}^{\mathrm{N}}\, P(N) \equiv \int \mathrm{d}^2Y^1 \int \mathrm{d}^2Y^2 \cdots \int \mathrm{d}^2Y^{\mathrm{N}}\, P(N), \tag{12}$$

where an abbreviated notation has been introduced to indicate integration over all possible positions of the irregularities on S_s. The restriction to equal irregularities, that has been introduced only for simplicity, can easily be removed by enlarging the probability space over which P is defined to include additional parameters characterizing the irregularities such as size, orientation and others.

The reduced probability distribution in which the position of K irregularities is prescribed is obtained from $P(N)$ by integration

$$P(K) = \frac{1}{(N-K)!} \int \mathrm{d}\mathcal{C}^{N-K} P(N), \tag{13}$$

and satisfies the normalization condition

$$\int \mathrm{d}\mathcal{C}^K\, P(K) = \frac{N!}{(N-K)!}. \tag{14}$$

The conditional probability $P(N-K|K)$ for the arrangement $\mathcal{C}^{N-K}$ of $N-K$ particles, given that K particles have the arrangement $\mathcal{C}^K$, is defined by

$$P(N-K|K)P(K) = P(N). \tag{15}$$

From (12) and (14) one finds the normalization condition

$$\int \mathrm{d}\mathcal{C}^{N-K}\, P(N-K|K) = (N-K)!. \tag{16}$$

We can now define the unconditional average of the field ϕ by

$$\langle\phi\rangle(\boldsymbol{x}) = \frac{1}{N!} \int \mathrm{d}\mathcal{C}^{\mathrm{N}}\, P(N)\phi(\boldsymbol{x}|N), \tag{17}$$

where the notation $\phi(\boldsymbol{x}|N)$ stresses the dependence of the exact ϕ not only on the point $\boldsymbol{x}$, but also on the configuration of the N irregularities. Similarly, we introduce conditional averages by writing

$$\langle\phi\rangle_K(\boldsymbol{x}|K) = \frac{1}{(N-K)!} \int \mathrm{d}\mathcal{C}^{N-K}\, P(N-K|K)\phi(\boldsymbol{x}|N), \tag{18}$$

with a similar definition for the conditional averages of other quantities of interest.

4. Averaged formulation

We now average the problem stated in § 2 over the ensemble described by $P(N)$. Upon substitution of the decomposition (4) of ϕ into the definition (17), one finds

$$\langle\phi\rangle(\boldsymbol{x}) = \phi_0(\boldsymbol{x}) + \sum_{\alpha=1}^{\mathrm{N}} \frac{1}{N!} \int \mathrm{d}\mathcal{C}^{\mathrm{N}}\, P(N)\chi^\alpha(\boldsymbol{x}|N). \tag{19}$$

In computing the integral it should be recalled that χ^α has been defined to vanish when $\boldsymbol{x}$ is inside the boss α. Since the bosses are indistinguishable, all the N terms in the sum give the same contribution, equal to that of, say, boss α, with α arbitrary, so that

$$\begin{aligned}\langle\phi\rangle(\boldsymbol{x}) &= \phi_0(\boldsymbol{x}) + \frac{1}{(N-1)!}\int \mathrm{d}^2Y^\alpha\, P(\alpha) \int \mathrm{d}\mathcal{C}^{N-1}\, P(N-1|\alpha)\chi^\alpha, \\ &= \phi_0(\boldsymbol{x}) + \int \mathrm{d}^2Y^\alpha\, P(\alpha)\langle\chi^\alpha\rangle_1(\boldsymbol{x}|\alpha). \end{aligned} \tag{20}$$

Here we have used the definition (18) of conditional average:

$$\langle\chi^\alpha\rangle_1(\boldsymbol{x}|\alpha) = \frac{1}{(N-1)!}\int \mathrm{d}\mathcal{C}^{N-1}\, P(N-1|\alpha)\chi^\alpha(\boldsymbol{x}|N). \tag{21}$$

The problem satisfied by $\langle\chi^\alpha\rangle_1(\boldsymbol{x}|\alpha)$ is readily obtained from the exact formulation given in § 2 by averaging according to (21). Specifically, one finds

$$\nabla^2\langle\chi^\alpha\rangle_1 = 0, \tag{22}$$

with $\langle\chi^\alpha\rangle_1 \to 0$ at infinity and subject to (7) on $S_{\mathrm{s}} - \sigma^\alpha$ and either

$$\langle\chi^\alpha\rangle_1 = -\langle\psi^\alpha\rangle_1 \tag{23}$$

or

$$\boldsymbol{n}^\alpha \cdot \nabla\langle\chi^\alpha\rangle_1 = -\boldsymbol{n}^\alpha \cdot \nabla\langle\psi^\alpha\rangle_1 \tag{24}$$

on B^α.

At this point one encounters the difficulty inherent in all averaging approaches, namely that the mathematical problem for the averaged quantities is not closed. Indeed, upon calculating $\langle\psi^\alpha\rangle_1$ according to definition (18) with $K=1$, it is readily found that

$$\langle\psi^\alpha\rangle_1(\boldsymbol{x}|\alpha) = \phi_0 + \int \mathrm{d}Y^\beta\, P(\beta|\alpha)\langle\chi^\beta\rangle_2(\boldsymbol{x}|\alpha\beta), \tag{25}$$

where now configurations such that $\boldsymbol{x}$ is inside another boss β contribute nothing by definition of χ^β, and $\langle\chi^\beta\rangle_2$ is given by (18) with $K=2$.

5. The effective boundary condition

It is possible to derive a formal expression for the effective boundary condition on S_{s} without solving explicitly the problem posed in the previous section. We show the procedure in detail for the Dirichlet problem, and then give an abbreviated treatment of the Neumann problem.

(a) Dirichlet problem

Let $G^{\mathrm{D}}(\boldsymbol{x},\boldsymbol{y})$ be the (exact) Green's function appropriate for the Dirichlet problem in the domain bounded by S_{s} and $\partial\Omega_{\mathrm{s}}$. The general theory of Green's functions ensures that $G^{\mathrm{D}}(\boldsymbol{x},\boldsymbol{y}) = G^{\mathrm{D}}(\boldsymbol{y},\boldsymbol{x})$ and that $G^{\mathrm{D}} = 0$ when either $\boldsymbol{x}$ or $\boldsymbol{y}$ are on S_{s}. In view of this property, and of the condition $\langle\chi^\alpha\rangle_1 = 0$ on $S_{\mathrm{s}} - \sigma^\alpha$, Green's identity for $\langle\chi^\alpha\rangle_1$ reduces to

$$\langle\chi^\alpha\rangle_1(\boldsymbol{x}|\alpha) = \int_{B^\alpha} \mathrm{d}B_y^\alpha\, G^{\mathrm{D}}(\boldsymbol{x},\boldsymbol{y})\frac{\partial\langle\chi^\alpha\rangle_1}{\partial n_y}(\boldsymbol{y}|\alpha) - \int_{B^\alpha} \mathrm{d}B_y^\alpha\, \langle\chi^\alpha\rangle_1(\boldsymbol{y}|\alpha)\frac{\partial G^{\mathrm{D}}}{\partial n_y}(\boldsymbol{x},\boldsymbol{y}), \tag{26}$$

where the integrals are over the surface B^α of the αth boss. We now apply the standard procedure to express $\langle\chi^\alpha\rangle_1$ in terms of a single layer (see, for example, Stakgold 1979, p. 514, or Kress 1989, p. 69). Since the bosses do not overlap, the 'incident' field $\langle\psi^\alpha\rangle_1$ is harmonic and non-singular in the closed domain bounded by the surface B^α of the irregularity and the underlying portion σ^α of S_{s}. Green's identity written for the same point $\boldsymbol{x}$ appearing in (26) and the closed surface $\sigma^\alpha \bigcup B^\alpha$ therefore reduces to

$$0 = \int_{B^\alpha} \mathrm{d}B_y^\alpha\, G^{\mathrm{D}}(\boldsymbol{x},\boldsymbol{y})\frac{\partial\langle\psi^\alpha\rangle_1}{\partial n_y}(\boldsymbol{y}|\alpha) - \int_{B^\alpha} \mathrm{d}B_y^\alpha\, \langle\psi^\alpha\rangle_1(\boldsymbol{y}|\alpha)\frac{\partial G^{\mathrm{D}}}{\partial n_y}(\boldsymbol{x},\boldsymbol{y}). \tag{27}$$

The left-hand side vanishes because $\boldsymbol{x}$ is outside the closed surface $\sigma^\alpha \bigcup B^\alpha$. The first integral does not contain a contribution from σ^α because G^{D} vanishes for $\boldsymbol{y}$ on S_{s}, and similarly for the second integral since $\psi^\alpha = 0$ on S_{s} from definition (8) and the conditions satisfied by ϕ_0 and the χ^β.

By adding (27) to (26) and recalling condition (23), we then find

$$\langle\chi^\alpha\rangle_1(\boldsymbol{x}|\alpha) - \int_{B^\alpha} \mathrm{d}B_y^\alpha\, G^{\mathrm{D}}(\boldsymbol{x},\boldsymbol{y})\frac{\partial\langle\chi^\alpha\rangle_1}{\partial n_y}(\boldsymbol{y}|\alpha) = \int_{B^\alpha} \mathrm{d}B_y^\alpha\, G^{\mathrm{D}}(\boldsymbol{x},\boldsymbol{y})\frac{\partial\langle\psi^\alpha\rangle_1}{\partial n_y}(\boldsymbol{y}|\alpha). \tag{28}$$

Equation (28) can be simplified considerably if we take the point $\boldsymbol{x}$ in an intermediate range far from the boss on the boss scale, while still close to S_{s} with respect to the surface radius of curvature, i.e. $a \ll |\boldsymbol{x} - \boldsymbol{y}^\alpha| \ll R_{\mathrm{s}}$. In the language of singular perturbations, this would be the 'matching region', and it is at this point that we explicitly use the postulated separation of scales between the bosses' size and the 'macroscopic' dimensions of S_{s}. Locally then, near $\boldsymbol{y}^\alpha$, we may write

$$G^{\mathrm{D}}(\boldsymbol{x},\boldsymbol{y}) = -\frac{1}{4\pi|\boldsymbol{x}-\boldsymbol{y}|} + \frac{1}{4\pi|\boldsymbol{x}-\boldsymbol{y}'|} + F^{\mathrm{D}}(\boldsymbol{x},\boldsymbol{y}), \tag{29}$$

where $\boldsymbol{y}'$ is the image of $\boldsymbol{y}$ in the plane tangent to S_{s} at $\boldsymbol{y}^\alpha$ and F^{D} is regular and harmonic everywhere away from S_{s} and very nearly vanishes in the neighbourhood of B^α. (By $\boldsymbol{y}^\alpha$ we indicate the position vector of the centre of σ^α in three-dimensional space. The notation $\boldsymbol{Y}^\alpha$ is used instead for the position of the same point expressed in terms of curvilinear coordinates on the surface S_{s}.) For $\boldsymbol{x}$ in this intermediate range, $1/|\boldsymbol{x}-\boldsymbol{y}|$ and $1/|\boldsymbol{x}-\boldsymbol{y}'|$ are much larger than F. (Note that this approximation is not related to the density of irregularities on the rough surface, but only to the postulated smallness of the ratio of the boss scale to the radius of curvature of S_{s}.) Hence, an expansion of G^{D} in a Taylor series centred at $\boldsymbol{y}^\alpha$ gives

$$G^{\mathrm{D}}(\boldsymbol{x},\boldsymbol{y}) \simeq G^{\mathrm{D}}(\boldsymbol{x},\boldsymbol{y}^\alpha) + (\boldsymbol{y}-\boldsymbol{y}^\alpha)\cdot\nabla_y G^{\mathrm{D}}(\boldsymbol{x},\boldsymbol{y}^\alpha) + \cdots. \tag{30}$$

However, G^{D} vanishes on S_{s} and, for the same reason, of its first derivatives only the normal one is non-zero at $\boldsymbol{y}^\alpha$. Hence

$$G^{\mathrm{D}}(\boldsymbol{x},\boldsymbol{y}) \simeq (\boldsymbol{y}-\boldsymbol{y}^\alpha)\cdot\nabla_y G^{\mathrm{D}}(\boldsymbol{x},\boldsymbol{y}^\alpha) = 2[\boldsymbol{N}\cdot(\boldsymbol{y}-\boldsymbol{y}^\alpha)]\boldsymbol{N}\cdot\nabla_y G(\boldsymbol{x},\boldsymbol{y}^\alpha), \tag{31}$$

where $G=-1/(4\pi|\boldsymbol{x}-\boldsymbol{y}|)$ is the free-space Green's function. The factor 2 is a direct consequence of the image point in (29). We thus approximately find from the integral equation (28)

$$\langle\chi^\alpha\rangle_1(\boldsymbol{x}) \simeq 2(\mathcal{K}^\alpha+\mathcal{P}^\alpha)\boldsymbol{N}\cdot\nabla_y G(\boldsymbol{x},\boldsymbol{y}^\alpha), \tag{32}$$

where

$$\mathcal{K}^\alpha(\langle\chi^\alpha\rangle_1) = \int_{B^\alpha} \mathrm{d}B_y^\alpha\, \boldsymbol{N}\cdot(\boldsymbol{y}-\boldsymbol{y}^\alpha)\frac{\partial\langle\chi^\alpha\rangle_1}{\partial n_y}(\boldsymbol{y}|\alpha), \tag{33}$$

$$\mathcal{P}^\alpha(\langle\psi^\alpha\rangle_1) = \int_{B^\alpha} \mathrm{d}B_y^\alpha\, \boldsymbol{N}\cdot(\boldsymbol{y}-\boldsymbol{y}^\alpha)\frac{\partial\langle\psi^\alpha\rangle_1}{\partial n_y}(\boldsymbol{y}|\alpha), \tag{34}$$

are linear functionals of their arguments. It may also be noted that, from (9),

$$\mathcal{K}^\alpha+\mathcal{P}^\alpha = \int_{B^\alpha} \mathrm{d}B_y^\alpha\, \boldsymbol{N}\cdot(\boldsymbol{y}-\boldsymbol{y}^\alpha)\frac{\partial\langle\phi\rangle_1}{\partial n_y}(\boldsymbol{y}|\alpha). \tag{35}$$

By inserting (32) into the expression (20) for the average field we have

$$\langle\phi\rangle(\boldsymbol{x}) = \phi_0 + 2\int_{S_{\mathrm{s}}} \mathrm{d}^2Y^\alpha\, P(\alpha)(\mathcal{K}^\alpha+\mathcal{P}^\alpha)\boldsymbol{N}\cdot\nabla_y G(\boldsymbol{x},\boldsymbol{y}^\alpha). \tag{36}$$

This relation shows that the effect of the bosses is represented by a suitable distribution of dipoles over the surface S_{s}. We now take an 'inner limit' of (36) by letting the field point $\boldsymbol{x}$ approach S_{s} and use a standard result of potential theory (Kress 1989, p. 68; Stakgold 1979, p. 512) to find

$$\langle\phi\rangle(\boldsymbol{x})|_{S_{\mathrm{s}}} = -P(\boldsymbol{x})(\mathcal{K}+\mathcal{P}) + \int_{S_{\mathrm{s}}} d^2Y^\alpha P(\alpha)(\mathcal{K}^\alpha+\mathcal{P}^\alpha)\frac{\boldsymbol{N}\cdot(\boldsymbol{y}^\alpha-\boldsymbol{x})}{|\boldsymbol{y}^\alpha-\boldsymbol{x}|^3}, \tag{37}$$

where we have dropped the superscript α in this term as $\mathcal{K}$ and $\mathcal{P}$ in the first term are to be evaluated for the boss centred at $\boldsymbol{x}\in S_{\mathrm{s}}$. The integral, in which $\boldsymbol{y}^\alpha$ is the position vector in space of the point having the surface curvilinear coordinates $\boldsymbol{Y}^\alpha$, is now regular. If S_{s} is plane, this integral vanishes identically due to the orthogonality of $\boldsymbol{N}$ and $\boldsymbol{y}^\alpha-\boldsymbol{x}$. If the radius of curvature is large, as postulated here, its contribution will be small and (37) gives the effective boundary condition

$$\langle\phi\rangle(\boldsymbol{x})|_{S_{\mathrm{s}}} = -P(\boldsymbol{x})[\mathcal{K}+\mathcal{P}], \tag{38}$$

or, from (35),

$$\langle\phi\rangle(\boldsymbol{x})|_{S_{\mathrm{s}}} = -P(\boldsymbol{x})\int_B \mathrm{d}B_y\, \boldsymbol{N}\cdot(\boldsymbol{y}-\boldsymbol{x})\frac{\partial\langle\phi\rangle_1}{\partial n_y}(\boldsymbol{y}|\boldsymbol{x}). \tag{39}$$

This relation explicitly shows the dependence of $\langle\phi\rangle$ on $\langle\phi\rangle_1$.

(b) *Neumann problem*

We now denote by G^{N} the exact Green's function for the Neumann problem in the domain bounded by S_{s} and $\partial\Omega_{\mathrm{s}}$. By following steps similar to those leading from

(26) to (28) (see, for example, Stakgold 1979) we find, in place of (28),

$$\langle\chi^\alpha\rangle_1(\boldsymbol{x}|\alpha)+\int_{B^\alpha}\mathrm{d}B^\alpha_y\,\langle\chi^\alpha\rangle_1(\boldsymbol{y}|\alpha)\frac{\partial G^{\mathrm{N}}}{\partial n_y}(\boldsymbol{x},\boldsymbol{y})=-\int_{B^\alpha}\mathrm{d}B^\alpha_y\,\langle\psi^\alpha\rangle_1(\boldsymbol{y}|\alpha)\frac{\partial G^{\mathrm{N}}}{\partial n_y}(\boldsymbol{x},\boldsymbol{y}).\tag{40}$$

In this case, the form of G^{N} in the matching region is

$$G^{\mathrm{N}}(\boldsymbol{x},\boldsymbol{y})=-\frac{1}{4\pi|\boldsymbol{x}-\boldsymbol{y}|}-\frac{1}{4\pi|\boldsymbol{x}-\boldsymbol{y}'|}+F^{\mathrm{N}}(\boldsymbol{x},\boldsymbol{y}),\tag{41}$$

where, as before, $\boldsymbol{y}'$ is the image of $\boldsymbol{y}$ in the plane tangent to S_{s} at $\boldsymbol{y}^\alpha$ and $\boldsymbol{N}\cdot\nabla F^{\mathrm{N}}$ very nearly vanishes on S_{s} and is regular and harmonic everywhere away from S_{s}. An expansion similar to (30) now gives

$$\boldsymbol{n}^\alpha\cdot\nabla G^{\mathrm{N}}(\boldsymbol{x},\boldsymbol{y})\simeq 2\boldsymbol{n}^\alpha\cdot\nabla_H G(\boldsymbol{x},\boldsymbol{y}^\alpha),\tag{42}$$

where G, as before, is the free-space Green's function, and ∇_H denotes the projection of the gradient on the tangent plane at $\boldsymbol{y}^\alpha$. The appearance of ∇_H rather than ∇ is a consequence of the fact that $\boldsymbol{N}\cdot\nabla G^{\mathrm{N}}=0$ on the plane. Upon substitution into (40) we may thus write

$$\langle\chi^\alpha\rangle_1\simeq -2(\boldsymbol{k}^\alpha+\boldsymbol{p}^\alpha)\cdot\nabla_H G,\tag{43}$$

where

$$\boldsymbol{k}^\alpha=\int_{B^\alpha}\mathrm{d}B^\alpha_y\,\langle\chi^\alpha\rangle_1(\boldsymbol{y}|\alpha)[\boldsymbol{n}^\alpha-\boldsymbol{N}(\boldsymbol{n}^\alpha\cdot\boldsymbol{N})],\tag{44}$$

$$\boldsymbol{p}^\alpha=\int_{B^\alpha}\mathrm{d}B^\alpha_y\,\langle\psi^\alpha\rangle_1(\boldsymbol{y}|\alpha)[\boldsymbol{n}^\alpha-\boldsymbol{N}(\boldsymbol{n}^\alpha\cdot\boldsymbol{N})].\tag{45}$$

The subtraction of the second term in the integrands removes the component normal to the tangent plane that is not required as is clear from (43).

Upon substitution into (20) we find

$$\begin{aligned}\langle\phi\rangle(\boldsymbol{x})&=\phi_0-2\int_{S_{\mathrm{s}}}\mathrm{d}^2Y^\alpha\,P(\alpha)(\boldsymbol{k}^\alpha+\boldsymbol{p}^\alpha)\cdot\nabla_H G\\&=\phi_0-2\int_{S_{\mathrm{s}}}\mathrm{d}^2Y^\alpha\,\nabla_H\cdot[P(\alpha)(\boldsymbol{k}^\alpha+\boldsymbol{p}^\alpha)G]\\&\quad+2\int_{S_{\mathrm{s}}}\mathrm{d}^2Y^\alpha\,G\nabla_H\cdot[P(\alpha)(\boldsymbol{k}^\alpha+\boldsymbol{p}^\alpha)].\end{aligned}\tag{46}$$

After eliminating the first integral by using the divergence theorem and assuming a vanishing contribution from the bounding curve, we recognize that the effect of the bosses is represented by the distribution of suitable sources on S_{s}. Upon taking the normal derivative and evaluating it on S_{s} we have then, since $\boldsymbol{N}\cdot\nabla\phi_0$ vanishes by definition,

$$\boldsymbol{N}\cdot\nabla\langle\phi\rangle=2\int_{S_{\mathrm{s}}}\mathrm{d}^2Y^\alpha\,(\boldsymbol{N}\cdot\nabla_x G)\nabla_H\cdot[P(\alpha)(\boldsymbol{k}^\alpha+\boldsymbol{p}^\alpha)].\tag{47}$$

The same step leading from (36) to (38) gives now

$$\boldsymbol{N}\cdot\nabla\langle\phi\rangle|_{S_{\mathrm{s}}}=\nabla_H\cdot\{P(\boldsymbol{x})(\boldsymbol{k}+\boldsymbol{p})\},\tag{48}$$

which is the effective boundary condition for the Neumann problem. The regular integral analogous to that of (37) has already been discarded here and $\boldsymbol{k}$ and $\boldsymbol{p}$ are to be evaluated for the boss centred at $\boldsymbol{x}$.

Equations (38) and (48) are the general form of the effective boundary conditions for the Dirichlet and Neumann problems, respectively. In order to render them fully explicit, we need expressions for the quantities $\mathcal{K}$, $\mathcal{P}$, $\boldsymbol{k}$ and $\boldsymbol{p}$. This task is accomplished for the dilute limit in the next section. For the Dirichlet problem, we address numerically the case of finite concentrations in § 8.

6. The first-order problem

We now obtain explicit expressions for the effective boundary condition in the dilute limit, i.e. to first order in the area fraction covered by the bosses.

(a) *The Dirichlet problem*

For the Dirichlet problem we start by noting that, since ψ^α accounts for the effect of all the other bosses on the boss located at $\boldsymbol{y}^\alpha$, $\langle\psi^\alpha\rangle_1$ is slowly varying near $\boldsymbol{y}^\alpha$ so that, on B^α, we may write

$$\langle\psi^\alpha\rangle_1(\boldsymbol{y}) = (\boldsymbol{y}-\boldsymbol{y}^\alpha)\cdot\nabla\langle\psi^\alpha\rangle_1(\boldsymbol{y}^\alpha) + \cdots. \tag{49}$$

Here we have used the fact that, since bosses cannot overlap, $\langle\psi^\alpha\rangle_1$ vanishes by definition on the base σ^α of the αth boss. For the same reason, only the normal component of the gradient can be non-zero so that on B^α, approximately,

$$\frac{\partial\langle\psi^\alpha\rangle_1}{\partial n_y}(\boldsymbol{y}|\alpha) \simeq (\boldsymbol{n}\cdot\boldsymbol{N})[\boldsymbol{N}\cdot\nabla\langle\psi^\alpha\rangle_1(\boldsymbol{y}^\alpha)]. \tag{50}$$

Upon substitution into definition (34) of $\mathcal{P}$, we then find

$$\mathcal{P}^\alpha(\langle\psi^\alpha\rangle_1) \simeq V^\alpha[\boldsymbol{N}\cdot\nabla\langle\psi^\alpha\rangle_1(\boldsymbol{y}^\alpha)], \tag{51}$$

where V^α, a constant only dependent on the geometry of the boss, is given by

$$V^\alpha = \int_{B^\alpha} \mathrm{d}B_y^\alpha\,[\boldsymbol{N}\cdot(\boldsymbol{y}-\boldsymbol{y}^\alpha)](\boldsymbol{N}\cdot\boldsymbol{n}). \tag{52}$$

A straightforward application of the divergence theorem shows that V^α is nothing other than the volume of the boss. If L denotes the characteristic length scale for the variation of $\langle\psi^\alpha\rangle_1$, the relative error in (51) is of the order of $(a/L)^2$.

We now turn to the problem (22), (23) for $\langle\chi^\alpha\rangle_1$. Again we use the slow variation of $\langle\psi^\alpha\rangle_1$ and (49) to write the boundary condition (23) in the approximate form

$$\langle\chi^\alpha\rangle_1(\boldsymbol{x}) \simeq -[(\boldsymbol{x}-\boldsymbol{y}^\alpha)\cdot\boldsymbol{N}][\boldsymbol{N}\cdot\nabla\langle\psi^\alpha\rangle_1(\boldsymbol{y}^\alpha|\alpha)]. \tag{53}$$

In view of the linearity of the problem, it is evident that the solution of (22) subject to this boundary condition will have the form

$$\langle\chi^\alpha\rangle_1(\boldsymbol{x}) = X(\boldsymbol{x}-\boldsymbol{y}^\alpha)\boldsymbol{N}\cdot\nabla\langle\psi^\alpha\rangle_1(\boldsymbol{y}^\alpha|\alpha), \tag{54}$$

for a suitable harmonic function $X(\boldsymbol{x}-\boldsymbol{y}^\alpha)$ dependent only on the geometry of the boss and satisfying, on the boss's surface,

$$X(\boldsymbol{x}) = -\boldsymbol{N}\cdot\boldsymbol{x}. \tag{55}$$

Hence, the quantity $\mathcal{K}^\alpha$ defined in (33) may be written

$$\mathcal{K}^\alpha = V^\alpha k^\alpha \boldsymbol{N}\cdot\nabla\langle\psi^\alpha\rangle_1(\boldsymbol{y}^\alpha|\alpha), \tag{56}$$

in which

$$k^\alpha = \frac{1}{V^\alpha}\int_{B^\alpha} \mathrm{d}B_y^\alpha\, \boldsymbol{N}\cdot(\boldsymbol{y}-\boldsymbol{y}^\alpha)\frac{\partial X}{\partial n_y}(\boldsymbol{y}-\boldsymbol{y}^\alpha). \tag{57}$$

Upon substitution of these results into the form (38) of the effective boundary condition, we then find

$$\langle\phi\rangle(\boldsymbol{x}) = P(\boldsymbol{x})V(1+k)\boldsymbol{N}\cdot\nabla\langle\psi\rangle_1(\boldsymbol{x}|\boldsymbol{x}). \tag{58}$$

Upon recognizing that

$$P(\boldsymbol{x})V = C(\boldsymbol{x}) \tag{59}$$

is the volume occupied by the bosses per unit surface of S_s, we may also write

$$\langle\phi\rangle(\boldsymbol{x}) = -(1+k)C(\boldsymbol{x})\boldsymbol{N}\cdot\nabla\langle\psi\rangle_1(\boldsymbol{x}|\boldsymbol{x}). \tag{60}$$

This is still an incomplete result as the field $\langle\psi\rangle_1$ is not known. Since, however, this field appears here multiplied by a quantity of the first order in the boss concentration, it is consistent to use for it an approximation of zero-order accuracy. While one could use the 'incident' field ϕ_0, it is clearly more accurate to use the classic approximation introduced by Foldy (1945), namely

$$\langle\psi\rangle_1 \simeq \langle\phi\rangle, \tag{61}$$

so that the effective boundary condition (38) becomes

$$\langle\phi\rangle(\boldsymbol{x}) = -(1+k)C(\boldsymbol{x})\boldsymbol{N}\cdot\nabla\langle\phi\rangle(\boldsymbol{x}). \tag{62}$$

The original Dirichlet boundary condition is thus transformed into a mixed condition. A discussion of this result will be given in § 11 and values of k for some specific shapes will be calculated in § 7.

(b) The Neumann problem

For the Neumann problem, the expansion analogous to (49) is

$$\langle\psi^\alpha\rangle_1(\boldsymbol{y}) = \langle\psi^\alpha\rangle_1(\boldsymbol{y}^\alpha) + (\boldsymbol{y}-\boldsymbol{y}^\alpha)\cdot\nabla_H\langle\psi^\alpha\rangle_1(\boldsymbol{y}^\alpha) + \cdots, \tag{63}$$

where we have used the fact that $\boldsymbol{N}\cdot\langle\psi^\alpha\rangle_1$ vanishes on the base σ^α of the αth boss.

Upon substitution of (63) into the integral (45) defining $\boldsymbol{p}^\alpha$, it is readily found that the first term contributes nothing while, from the second term, one has

$$\boldsymbol{p}^\alpha \simeq V^\alpha\nabla_H\langle\psi^\alpha\rangle_1(\boldsymbol{y}^\alpha), \tag{64}$$

with a relative error of order $(a/L)^2$. This contribution is very similar to that found for the Dirichlet problem.

To calculate $\boldsymbol{k}^\alpha$ we need to solve the problem (22), (24) for $\langle\chi^\alpha\rangle_1$. Again we use the slow variation of $\langle\psi^\alpha\rangle_1$ and (63) to write the boundary condition (24) in the approximate form

$$\boldsymbol{n}^\alpha\cdot\nabla\langle\chi^\alpha\rangle_1 \simeq -\boldsymbol{n}^\alpha\cdot\nabla_H\langle\psi^\alpha\rangle_1(\boldsymbol{y}^\alpha|\alpha). \tag{65}$$

In this case the linearity of the problem entails that the required solution of (22) will have the form

$$\langle\chi^\alpha\rangle_1(\boldsymbol{x}|\boldsymbol{y}^\alpha) = [\boldsymbol{M}^\alpha(\boldsymbol{x}-\boldsymbol{y}^\alpha)]\cdot\nabla_H\langle\psi^\alpha\rangle_1(\boldsymbol{y}^\alpha|\alpha), \tag{66}$$

where $\boldsymbol{M}^\alpha$ is a vector in the tangent plane at $\boldsymbol{y}^\alpha$. Each one of its components satisfies the Laplace equation subject to $\boldsymbol{N}\cdot\nabla M_i^\alpha = 0$, $i=1,2$ on the plane, and, on B^α,

$$\boldsymbol{n}^\alpha\cdot\nabla M_i^\alpha = -\boldsymbol{n}^\alpha\cdot\boldsymbol{e}_i, \quad i=1,2, \tag{67}$$

where $\boldsymbol{e}_1$, $\boldsymbol{e}_2$ are a pair of orthogonal unit vectors in the plane and $\boldsymbol{n}^\alpha$ is the outward normal to the boss as before. With this relation the vector $\boldsymbol{k}^\alpha$ defined by (44) becomes

$$\boldsymbol{k}^\alpha = V^\alpha \mathcal{M}^\alpha \cdot \nabla_H \langle \psi^\alpha \rangle_1 (\boldsymbol{y}^\alpha | \alpha), \tag{68}$$

where the 2×2 tensor $\mathcal{M}$ only depends on the geometry of the bosses and is given by

$$\mathcal{M}^\alpha = \frac{1}{V^\alpha} \int_{\mathcal{B}^\alpha} \mathrm{d}B^\alpha \, n^\alpha \otimes (\boldsymbol{M}^\alpha)^{\mathrm{T}}, \tag{69}$$

where $\otimes$ denotes the outer product and the superscript T the transpose. It is readily shown that this tensor is symmetric. Indeed, from (69) and the boundary conditions (67), we may write

$$\mathcal{M}^\alpha_{ij} = -\frac{1}{V^\alpha} \int_{B^\alpha} \mathrm{d}B^\alpha \, M^\alpha_j (\nabla M^\alpha_i \cdot \boldsymbol{n}^\alpha). \tag{70}$$

The integral can be extended to the entire boundary of the problem because the normal gradient of $\boldsymbol{M}^\alpha$ vanishes on the smooth part of the boundary away from B^α and because $\boldsymbol{M}^\alpha$ vanishes at infinity. Application of Green's identity then proves the statement since the components of $\boldsymbol{M}^\alpha$ are harmonic. Furthermore, for axisymmetric bosses, $\mathcal{M}^\alpha$ is a multiple of the identity $\mathcal{I}$. To prove this statement, consider a rotation of the coordinate system around the axis of the boss. The components of $\mathcal{M}^\alpha$ in the new frame must equal those in the old frame because the mathematical problem is identical in the two frames. In view of the general transformation properties of vectors and tensors, we may then write

$$\mathcal{M}^\alpha = \mathcal{O} \mathcal{M}^\alpha \mathcal{O}^{\mathrm{T}} \tag{71}$$

for any orthogonal rotation matrix $\mathcal{O}$. As a consequence, $\mathcal{M} = m\mathcal{I}$.

Upon substitution of (64) and (68) into the form (48) of the effective boundary condition, we find

$$\boldsymbol{N} \cdot \nabla \langle \phi \rangle = \nabla_H \cdot [C(\mathcal{I} + \mathcal{M}) \cdot \nabla_H \langle \psi^\alpha \rangle_1 (\boldsymbol{x} | \boldsymbol{x})], \tag{72}$$

where C is the volume concentration of bosses per unit surface defined in (59). Adopting the same closure (61), this result takes the more explicit form

$$\boldsymbol{N} \cdot \nabla \langle \phi \rangle |_{S_s} = \nabla_H \cdot [C(\boldsymbol{x})(\mathcal{I} + \mathcal{M}) \cdot \nabla_H \langle \phi \rangle (\boldsymbol{x})]. \tag{73}$$

If the tensor $\mathcal{M}$ is a multiple of the identity and the boss concentration C uniform, since $\langle \phi \rangle$ is harmonic, we find the particular form

$$\frac{\partial \langle \phi \rangle}{\partial N} = -C(1+m) \frac{\partial^2 \langle \phi \rangle}{\partial N^2}, \tag{74}$$

where $\partial / \partial N$ is the derivative in the direction normal to the plane. Examples of the calculation of the constant m are given in the next section.

7. Examples

We now consider some specific cases in which the constants that enter the effective boundary conditions derived before can be calculated explicitly. The simplest case is that of a hemispherical boss. We also consider prolate and oblate hemispheroids, and bosses in the form of spherical segments.

Hemispherical bosses. Assume a coordinate system centred at the centre of the boss's base with the x_3-axis along the axis of symmetry of the boss. From (55) the function X required for the Dirichlet problem is evidently

$$X = -a^3 x_3 / r^3, \tag{75}$$

where r is the distance from the centre of the hemisphere, and a is the radius of the hemisphere. Therefore, for this case,

$$k = -3 \int_0^{\pi/2} \cos\theta (2\cos\theta) \, \mathrm{d}\cos\theta = 2. \tag{76}$$

The Dirichlet effective boundary condition (62) then becomes

$$\langle\phi\rangle(\boldsymbol{x}) = -3C(\boldsymbol{x})\boldsymbol{N} \cdot \nabla\langle\phi\rangle(\boldsymbol{x}). \tag{77}$$

Similarly, for the Neumann problem, we have

$$\boldsymbol{M} = \tfrac{1}{2} a^3 (\boldsymbol{x} - \boldsymbol{y})_{\|} / r^3, \tag{78}$$

where the subscript $\|$ indicates the component parallel to the plane. A straightforward calculation confirms the tensor $\mathcal{M}$ to be a multiple of the identity with

$$m = \tfrac{1}{2}. \tag{79}$$

The effective boundary condition is then

$$\boldsymbol{N} \cdot \nabla\langle\phi\rangle = \tfrac{3}{2} \nabla_H \cdot [C(\boldsymbol{x}) \nabla_H \langle\phi\rangle]. \tag{80}$$

Prolate and oblate spheroids. The determination of X and $\boldsymbol{M}$ is similar for the case of bosses having the shape of oblate or prolate hemispheroids. Now oblate and prolate spheroidal coordinates are convenient. The detailed calculations are given in the Appendix.

Denote by Λ the aspect ratio of the spheroids,

$$\Lambda = b/a, \tag{81}$$

where a and b are the axes in the direction parallel and perpendicular to the plane. For the oblate case $\Lambda < 1$, while $\Lambda > 1$ in the prolate case. Then, for the Dirichlet problem, we find

$$k = -\frac{\Lambda^{-2} \arctan\left(\sqrt{\Lambda^{-2} - 1}\right) - \sqrt{\Lambda^{-2} - 1}}{\Lambda^{-2} \left[\arctan\left(\sqrt{\Lambda^{-2} - 1}\right) - \sqrt{\Lambda^{-2} - 1}\right]}, \tag{82}$$

for both the oblate and prolate cases since $\tan \mathrm{i}u = \mathrm{i} \tanh u$.

For the Neumann problem $\mathcal{M} = m\mathcal{I}$ is a multiple of the identity with

$$m = \frac{\Lambda^{-2} \arctan\left(\sqrt{\Lambda^{-2} - 1}\right) - \sqrt{\Lambda^{-2} - 1}}{\Lambda^{-2} \arctan\left(\sqrt{\Lambda^{-2} - 1}\right) + \sqrt{\Lambda^{-2} - 1}(1 - 2\Lambda^{-2})}, \tag{83}$$

valid again for both the oblate and prolate cases.

The quantity $1 + k$ is shown as a function of the aspect ratio by the dotted curve in figure 3. The dashed curve is the corresponding result $1 + m$ for the Neumann problem.

Spherical caps. For spherical caps we define the aspect ratio Λ as the height above

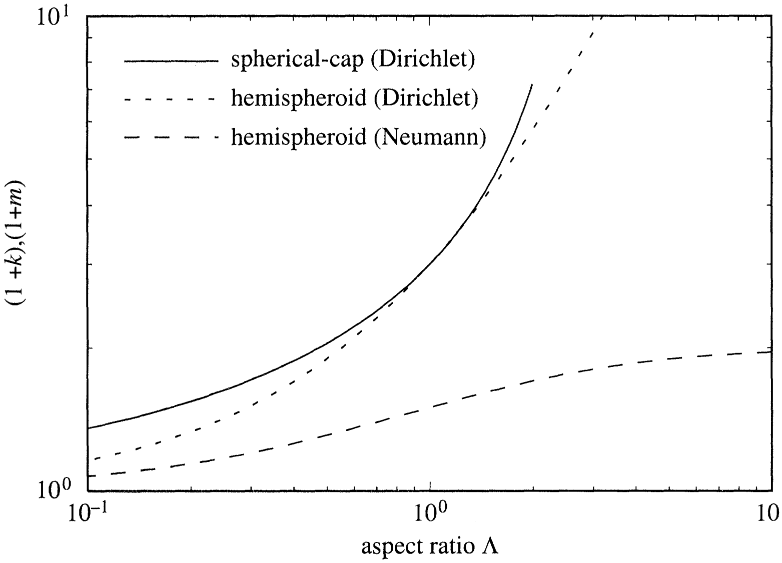

Figure 3. Graph of the quantities $1+k$ and $1+m$ defined in (57) and (69) as a function of the aspect ratio in the dilute case. The dotted and full curves show $1+k$ for spheroidal and spherical-segment bosses, respectively. The dashed curve shows $1+m$ for spheroidal bosses. For the spheroidal case, the aspect ratio is the height divided by the radius of the base. For spherical segments, the aspect ratio is the height divided by the radius of the sphere.

the surface divided by the sphere's radius. Clearly, with this definition, $0 \leqslant \Lambda \leqslant 2$. In this case the constant k for the Dirichlet problem is

$$k = \frac{8\pi a^3}{V} \int_0^\infty \frac{\sinh(\pi - \eta_0)\tau}{\cosh \pi\tau} \times \left[\frac{\tau^2}{\sinh \eta_0 \tau} + \frac{\tau \sinh(\pi - \eta_0)\tau \cot \eta_0 - 2\tau^2 \cosh(\pi - \eta_0)\tau}{3 \sinh \pi\tau} \right] \mathrm{d}\tau, \tag{84}$$

where

$$\cos \eta_0 = \Lambda - 1. \tag{85}$$

For the case of a hemisphere $\eta_0 = \frac{1}{2}\pi$ and $k = 2$ as before. The quantity $1+k$ is shown as a function of the aspect ratio by the solid curve in figure 3. Upon comparing with the spheroidal case it is seen that the results are not very sensitive to the shape.

We have been unable to find a comparable analytic expression for the constant m of the Neumann problem. The difficulty arises in the inversion of the Mehler–Fock transform necessary to impose the boundary conditions on the surface of the boss.

8. The Dirichlet problem at finite concentrations

While analytic results to second order in the boss concentration can probably be found, it does not seem possible to go to arbitrary concentrations by analytical means. Hence, we now treat the Dirichlet problem for hemispherical bosses numerically. In addition to its intrinsic interest, the numerical solution is also useful to gauge the domain of validity of the dilute calculations of the previous section.

In the absence of surface irregularities, a Taylor series expansion of ϕ near the boundary S_s would start with a term proportional to the distance from S_s as $\nabla_H \phi = 0$

on S_s. In the presence of irregularities, $\langle\phi\rangle$ does not necessarily vanish on the surface. However, for a uniform distribution of bosses as the one to be considered in this section, equation (38) shows that its horizontal gradient still vanishes. In this case, therefore, far from the surface in terms of the boss's size, but near it on the scale of the other 'macroscopic' lengths characterizing $\langle\phi\rangle$, we expect a structure of the form

$$\phi(\boldsymbol{x}) \simeq B(x_3 - D), \tag{86}$$

where x_3 is the perpendicular distance from S_s. This 'local' expression is equivalent to the effective boundary condition on the tangent plane $x_3 = 0$

$$\phi = -D\boldsymbol{N} \cdot \nabla\phi. \tag{87}$$

Since $D = 0$ for a smooth surface, D must depend upon the boss concentration. This fact will be clearly seen from the analysis that follows. In view of the linearity of the problem we can also assume $B = 1$.

To solve the problem we make the following remark. Let Φ be the solution of Laplace's equation in the whole space outside an infinity of spheres with their centres on the plane $x_3 = 0$, vanishing on the surface of the spheres, and asymptotic to x_3 as $x_3 \rightarrow \pm\infty$. Then, in the half-space $x_3 \geqslant 0$, Φ coincides with the solution ϕ of the rough boundary problem that we are interested in. A powerful method for the calculation of Φ is available on the basis of the results of Sangani & Behl (1989) as explained below. This symmetry argument fails in the case of the Neumann problem which, for this reason, cannot be solved by the present technique.

The plan of the calculation is the following. We place the centres of N_B non-overlapping spheres at random in a square of side h, and then replicate copies of this unit cell infinitely many times to cover the plane. The fraction of area covered by the bosses is clearly

$$\beta = \pi a^2 N_B/h^2, \tag{88}$$

and the volume of bosses per unit area

$$C = \tfrac{2}{3}a\beta. \tag{89}$$

The rough surface constructed in this way is only random up to the scale h. The error due to this circumstance can be decreased by increasing h as discussed below. By randomly rearranging the spheres in the unit cell many times, we generate an ensemble of rough surfaces. The exact Dirichlet problem is then solved numerically for each one of these realizations of the rough boundary, and the constant D defined by (86) is obtained from each solution. From the average of all the Ds thus calculated, we then find the effective boundary condition sought. This procedure is legitimate as it will be clear from the following that, far from the rough surface, $\nabla\phi$ is a constant unit vector for all realizations so that D and $\nabla\langle\phi\rangle$ are uncorrelated.

(*a*) *Numerical method*

Following Ishii (1979), Sangani & Behl (1989) have studied the solution of the Laplace equation in unbounded space in the presence of an infinite plane square lattice of spheres. The system described before corresponds to the superposition of N_B such lattices. The solution for Φ can therefore be written down directly by superposing the solutions of Sangani & Behl (1989),

$$\Phi = x_3 + \sum_{\alpha=1}^{N_B}\sum_{n=1}^{\infty}\sum_{m=0}^{n}[A_{nm}^{\alpha}\partial_3^{n-m}\Delta_m + \tilde{A}_{nm}^{\alpha}\partial_3^{n-m}\tilde{\Delta}_m]\Psi(\boldsymbol{r} - \boldsymbol{r}^{\alpha}), \tag{90}$$

where

$$\partial_3 = \frac{\partial}{\partial x_3}, \tag{91}$$

$$\Delta_m = \left(\frac{\partial}{\partial \xi}\right)^m + \left(\frac{\partial}{\partial \eta}\right)^m,$$

$$\tilde{\Delta}_m = \mathrm{i}\left[\left(\frac{\partial}{\partial \xi}\right)^m - \left(\frac{\partial}{\partial \eta}\right)^m\right], \quad \xi = x_1 + \mathrm{i}x_2, \quad \eta = x_1 - \mathrm{i}x_2. \tag{92}$$

Here $\boldsymbol{r}^\alpha$, with $\alpha = 1, 2, \ldots, N_B$ are the position vectors of the bosses in the unit cell and the function Ψ satisfies

$$\nabla^2 \Psi(\boldsymbol{r}) = 4\pi \sum_{l} \delta(\boldsymbol{r} - \boldsymbol{r}^l), \tag{93}$$

where $\boldsymbol{r}^l$ are the lattice points

$$\boldsymbol{r}^l = h(l_1 \boldsymbol{e}_1 + l_2 \boldsymbol{e}_2), \quad l_{1,2} = 0, \pm 1, \pm 2, \pm 3, \ldots. \tag{94}$$

The function Ψ has been evaluated by Sangani & Behl (1989), to which the reader is referred for details. It is shown in Appendix B that, for $x_3 \to \infty$, Φ given by (90) is asymptotic to

$$\Phi \sim x_3 - \frac{4\pi}{h^2} \sum_{\alpha=0}^{N_B} A^\alpha_{10}, \tag{95}$$

so that the constant D defined in (86) is given by

$$D = \frac{4\pi}{h^2} \sum_{\alpha=0}^{N_B} A^\alpha_{10}. \tag{96}$$

In the notation of § 6 we thus have

$$1 + k = \frac{6}{a^3 N_B} \sum_{\alpha=0}^{N_B} A^\alpha_{10}. \tag{97}$$

In order to evaluate the constants A^α_{nm}, $\tilde{A}^\alpha_{mn}$, we use an alternative representation of Φ in the vicinity of each boss, namely

$$\Phi(\boldsymbol{r}) = \sum_{n=0}^{\infty} \sum_{m=0}^{n} \left[C^\alpha_{nm} + D^\alpha_{nm}\left(\frac{a}{r}\right)^{2n+1}\right] Y^m_n + \left[\tilde{C}^\alpha_{nm} + \tilde{D}^\alpha_{nm}\left(\frac{a}{r}\right)^{2n+1}\right] \tilde{Y}^m_n, \tag{98}$$

where

$$Y^m_n = \frac{1}{(n+m)!} r^n P^m_n(\cos\theta) \cos m\varphi, \quad \tilde{Y}^m_n = \frac{1}{(n+m)!} r^n P^m_n(\cos\theta) \sin m\varphi. \tag{99}$$

(r, θ, φ) are spherical coordinates centred at the centre $\boldsymbol{r}^\alpha$ of the αth boss. The requirement that the field at the surface of the αth boss vanish is satisfied if

$$C^\alpha_{nm} = -D^\alpha_{nm}, \quad \tilde{C}^\alpha_{nm} = -\tilde{D}^\alpha_{nm}. \tag{100}$$

Following Sangani & Behl (1989), we relate the constants D^α_{nm}, $\tilde{D}^\alpha_{nm}$ to A^α_{nm}, $\tilde{A}^\alpha_{mn}$ as follows. The terms of the local and global expansions that are singular at the centre of the αth boss are matched to find

$$D^{\alpha}_{nm}a^{2n+1} = \frac{(n+m)!(n-m)!(-1)^{n-m}}{2^{m-1}}A^{\alpha}_{nm},$$

$$\tilde{D}^{\alpha}_{nm}a^{2n+1} = \frac{(n+m)!(n-m)!(-1)^{n-m}}{2^{m-1}}\tilde{A}^{\alpha}_{nm}. \tag{101}$$

For the terms regular at $\boldsymbol{r}^{\alpha}$ we have

$$C^{\alpha}_{nm} = \epsilon_m(-2)^m\partial_3^{n-m}\Delta_m\Phi(\boldsymbol{r}^{\alpha})^{\text{reg}}, \quad \tilde{C}^{\alpha}_{nm} = \epsilon_m(-2)^m\partial_3^{n-m}\Delta_m\Phi(\boldsymbol{r}^{\alpha})^{\text{reg}}, \tag{102}$$

where $\epsilon_m = 1 - \frac{1}{2}\delta_{m0}$ and the superscript 'reg' indicates the regular part of the function obtained by removing the singularity at $\boldsymbol{r} = \boldsymbol{r}^{\alpha}$. In evaluating Φ in the right-hand side of these relations, the representation (90) should be used. The constants C^{α}_{nm}, $\tilde{C}^{\alpha}_{nm}$, D^{α}_{nm}, $\tilde{D}^{\alpha}_{nm}$ are readily eliminated to obtain a linear system involving only the A^{α}_{nm}, $\tilde{A}^{\alpha}_{nm}$.

Some further information on the implementation of this method are given in Appendix B. Sangani & Behl (1989) give a complete description.

(*b*) *Numerical implementation*

The numerical implementation of the previous method requires several approximations. In the first place, the infinite middle summation over n in (90) needs to be truncated to a finite number of singularities. We have run several tests with the hemispheres at various distances and also so close as to nearly touch, and we have concluded that a maximum value of $n = 5$ is sufficient. The method of Sangani & Behl also requires a summation over the lattice points $\boldsymbol{r}^{l}$ (see Appendix B). We have found that a maximum value of 3 for $|l_{1,2}|$ gives satisfactory accuracy up to a concentration very near the close-packing limit.

Another quantity to be chosen is the number N_B of spheres in the unit cell. Figure 4 shows the running average of the numerical results for $1+k$ as a function of the number of configurations used. The dotted curves are for $N_B = 9$, the full curves for $N_B = 16$ and the broken curves for $N_B = 20$. The area fractions considered are, from top to bottom, 5%, 10%, 20%, 30%, 40%, 50%, 60%, 70% and 75%. As expected, due to the greater 'freedom' in the centres' position, convergence is slower at the lower concentrations. This is illustrated for the case $\beta = 5\%$ in figure 5, where the running average up to 40 configurations is presented for nine (dotted curve) and 16 (full curve) spheres in the unit cell. In all cases the results for $1 + k$ presented below have been determined with 16 particles and 20 configurations, except for the 5% case for which 40 configurations were used.

As is evident from (88), for a given area fraction, increasing N_B has the effect of increasing the side h of the unit cell. Figure 4 also shows then that the present implementation is not significantly affected by the artificial periodicity of our pseudo-random surfaces.

To test our computer program, we first compared its results with those of a code kindly made available to us by Professor Sangani for the case of a single square lattice of side h. Then we used four interpenetrating lattices with sides $2h$ and made sure that the results were identical.

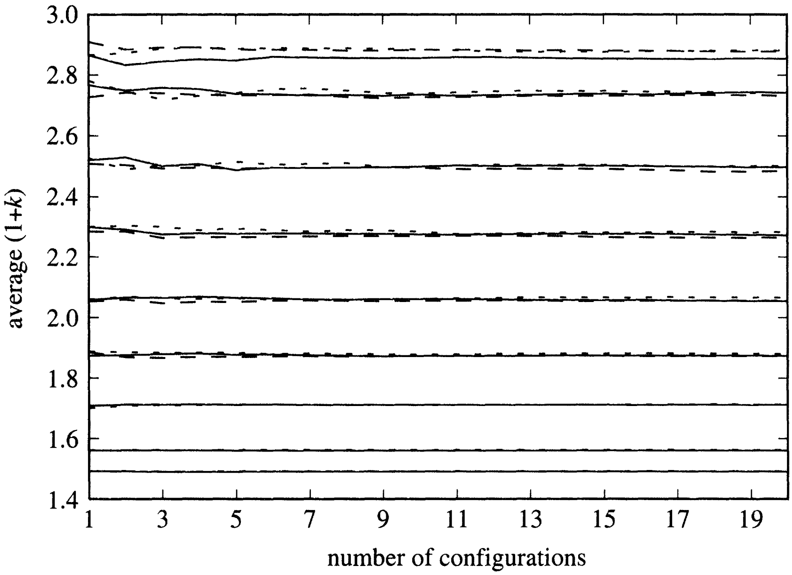

Figure 4. Running average of the numerical results for $1+k$ as a function of the number of configurations used in the direct numerical simulations at finite concentrations. The dotted curves are for a number N_B of particles in the fundamental cell equal to 9, the full curves for $N_B = 16$, and the dashed curves for $N_B = 20$. The area fractions considered are, from top to bottom, 5%, 10%, 20%, 30%, 40%, 50%, 60%, 70% and 75%.

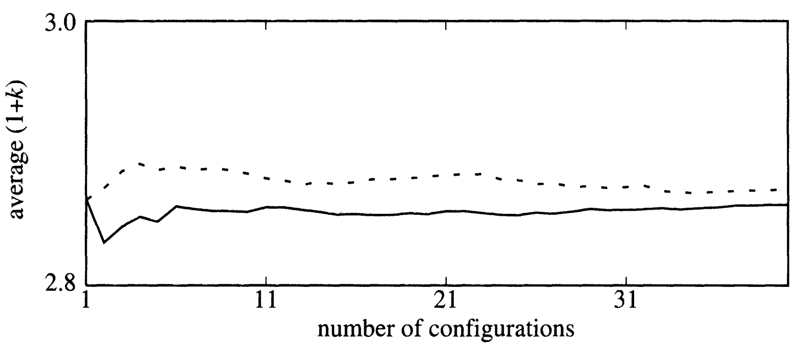

Figure 5. Running average of the numerical results for $1+k$ as a function of the number of configurations N used in the direct numerical simulations for an area coverage of 5%. The dotted curve is for a number N_B of particles in the fundamental cell equal to 9, the full curve for $N_B = 16$. The portion of the curves up to $N = 20$ is the same as that shown by the corresponding ones in figure 4.

(*c*) *Results*

The results of the numerical simulations are shown in figure 6. Here we plot the quantity $1+k$ appearing in the effective boundary condition (62)

$$\langle \phi \rangle = (1+k) C \boldsymbol{N} \cdot \nabla \langle \phi \rangle, \tag{103}$$

as a function of the area fraction β defined in (88). The curve starts at the dilute-limit value $1+k=3$ determined in the previous section and decreases monotonically. The maximum area fraction for a square lattice is $\frac{1}{4}\pi \simeq 0.785$. The simulations have been run up to $\beta = 75\%$. Over the range $0 \leqslant \beta \leqslant 75\%$ the curve in figure 6 is

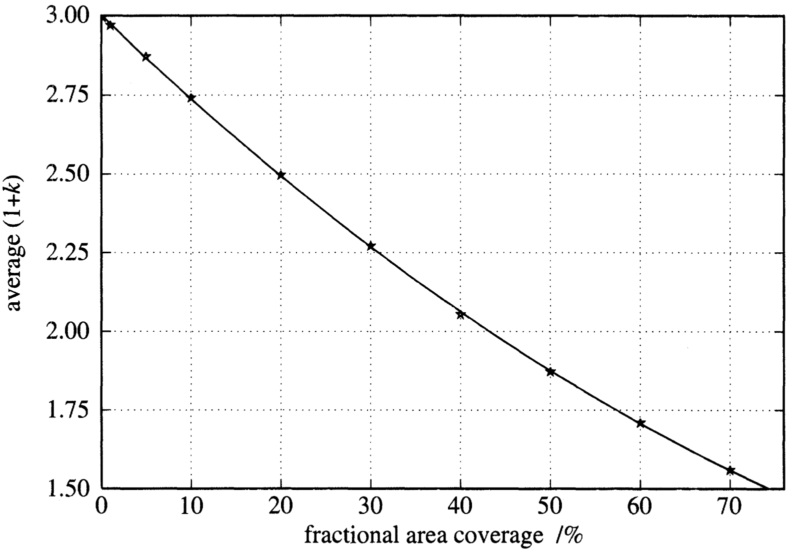

Figure 6. Graph of the quantity $1+k$ as a function of the fractional area coverage as obtained from the direct numerical simulation. The asterisks are the numerical results and the full curve the polynomial approximation (104).

closely reproduced by the simple polynomial

$$1+k = 3 - 2.7345\beta + 0.960\,22\beta^2, \tag{104}$$

that is also shown by the line in the figure.

9. The two-dimensional problem

The analysis of the two-dimensional problem proceeds in a very similar way and a very brief treatment will be sufficient. The term 'ridge' rather than 'boss' seems more appropriate in this case.

The results of § 5 remains valid provided the Green's function for the Dirichlet problem is taken as

$$G^{\mathrm{D}}(\boldsymbol{x},\boldsymbol{y}) = \frac{1}{2\pi}\log|\boldsymbol{x}-\boldsymbol{y}| - \frac{1}{2\pi}\log|\boldsymbol{x}-\boldsymbol{y}'| + F^{\mathrm{D}}(\boldsymbol{x},\boldsymbol{y}), \tag{105}$$

in place of (29). A Taylor-series expansion leads to the same expression (31) with $G = [1/(2\pi)]\log|\boldsymbol{x}-\boldsymbol{y}|$. The definitions (33) and (34) of $\mathcal{K}^\alpha$ and $\mathcal{P}^\alpha$ still hold with the integrals interpreted as line integrals over the trace of the ridge. The effective boundary condition (38) is formally applicable to this case as well.

The analysis of the dilute case proceeds as before with, in place of (56),

$$\mathcal{K}^\alpha = A^\alpha k^\alpha \boldsymbol{N}\cdot\nabla\langle\psi^\alpha\rangle_1(\boldsymbol{y}^\alpha|\alpha), \tag{106}$$

where A^α is the area of the ridge and (cf. (57))

$$k^\alpha = \frac{1}{A^\alpha}\int_{B^\alpha} \mathrm{d}B_y\,\boldsymbol{N}\cdot(\boldsymbol{y}-\boldsymbol{y}^\alpha)\frac{\partial X}{\partial n_y}(\boldsymbol{y}-\boldsymbol{y}^\alpha). \tag{107}$$

As before, the function X is harmonic and satisfies the boundary condition (55) on the ridge. The effective boundary condition (62) is also formally unchanged except that, in this case, $C(\boldsymbol{x}) = P(\boldsymbol{x})A$.

The situation is similar for the case of Neumann conditions. In particular, (48) still holds with the same formal expressions (44) and (45) for $\boldsymbol{k}^\alpha$ and $\boldsymbol{p}^\alpha$. In the dilute limit we have a result similar to (73) except that, since the tangent plane to S_s is replaced by a tangent line that we approximate with the x_1 axis,

$$\boldsymbol{N}\cdot\nabla\langle\phi\rangle = \frac{\partial}{\partial x_1}\left\{C(\boldsymbol{x})[1+m(\boldsymbol{x})]\frac{\partial}{\partial x_1}\langle\phi\rangle(\boldsymbol{x})\right\}. \tag{108}$$

Here

$$m = \frac{1}{A}\int_B \mathrm{d}B_y\, n_1 M, \tag{109}$$

where n_1 is the projection of the normal to the ridge onto the x_1-direction and M is harmonic and satisfies $\boldsymbol{n}\cdot\nabla M = -n_1$ on the surface of the ridge.

As an example, for cylindrical ridges with radius a, we readily find

$$X = -a^2\frac{x_3}{r^2}, \quad M = a^2\frac{x_1}{r^2}, \tag{110}$$

so that $k = m = 1$ and

$$\langle\phi\rangle(\boldsymbol{x}) = -2C(\boldsymbol{x})\boldsymbol{N}\cdot\nabla\langle\phi\rangle(\boldsymbol{x}) \tag{111}$$

for the Dirichlet case and

$$\boldsymbol{N}\cdot\nabla\langle\phi\rangle = 2\frac{\partial}{\partial x_1}\left[C(\boldsymbol{x})\frac{\partial}{\partial x_1}\langle\phi\rangle(\boldsymbol{x})\right] \tag{112}$$

for the Neumann case.

10. Applications

A few applications of the effective boundary conditions derived in the previous sections are useful to understand their physical content and to give a feeling for the differences that one may expect with respect to smooth surfaces.

Potential flow past a rough sphere. Consider a sphere of radius R immersed in a uniform flow with velocity U. The sphere's surface is characterized by a uniform distribution of roughnesses. According to (74), the condition of vanishing normal potential gradient over the rough surface is replaced by

$$\frac{\partial\phi}{\partial r} = -(1+m)C\frac{\partial^2\phi}{\partial r^2}, \tag{113}$$

where C is the boss volume per unit area and m is a constant dependent on the boss's shape. The potential-flow problem subject to this condition is readily solved to find

$$\phi = Ur\cos\theta\left[1+\frac{1}{1-3(1+m)C/R}\frac{R^3}{2r^3}\right]. \tag{114}$$

In particular, the added mass coefficient of the sphere is increased from the value $\frac{1}{2}$ for a smooth sphere to the value

$$\frac{1}{2}\frac{1}{[1-3(1+m)C/R]^2} \simeq \frac{1}{2}\left[1+6\frac{(1+m)C}{R}\right], \tag{115}$$

as if the sphere's radius were increased by the amount $2(1+m)C$.

Capacitance of a rough sphere. Let the electrostatic potential be V_0 far from a conducting sphere of radius R held at zero potential. According to equation (62), the exact boundary condition is replaced by

$$\phi = -(1+k)C\frac{\partial \phi}{\partial r}, \tag{116}$$

where k is a constant depending on the boss's shape. The capacitance is readily calculated to be

$$\mathcal{C} = \frac{4\pi R}{1-(1+k)C/R} \simeq 4\pi R\left[1+(1+k)\frac{C}{R}\right], \tag{117}$$

corresponding to an apparent increase of the sphere's radius by the amount $(1+k)C$.

Reflection of surface waves. Consider two-dimensional small-amplitude irrotational surface waves propagating on the surface of a liquid in a shallow channel. The channel bottom is smooth for $x<0$ and uniformly rough for $x>0$. The boundary condition at the bottom for $x>0$ is therefore, according to (74),

$$\frac{\partial \phi}{\partial z} = -(1+m)C\frac{\partial^2 \phi}{\partial z^2}. \tag{118}$$

The amplitudes of the reflected $\mathcal{R}$ and transmitted $\mathcal{T}$ waves, normalized by the incident wave, due to the discontinuity in boundary conditions at $x=0$ are given by the formulae

$$\mathcal{R} = \frac{k_+ - k_-}{k_+ + k_-}, \quad \mathcal{T} = \frac{2k_-}{k_+ + k_-}, \tag{119}$$

where $k_\pm$ are the wavenumbers for $x>0$ and $x<0$. To find these quantities we calculate the dispersion relations in the two regions finding, for $x<0$,

$$\omega^2 = gk_- \tanh hk_-, \tag{120}$$

and, for $x>0$,

$$\omega^2 = gk_+ \tanh \ell k_+, \tag{121}$$

where h is the undisturbed channel depth and ℓ is determined by

$$\tanh k_+(h-\ell) = (1+m)Ck_+. \tag{122}$$

With the assumption $(h-\ell)/h \ll 1$, this relation gives

$$\ell = h-(1+m)C. \tag{123}$$

It is therefore clear from (121) that the rough part of a channel behaves as if it were shallower than h by the amount $(1+m)C$. Upon equating (120) and (121), we find, for small $|k_+ - k_-|$,

$$k_+ = k_-\left[1+\frac{(1+m)C}{2h}\right], \tag{124}$$

so that, from(119),

$$\mathcal{R} \simeq \frac{(1+m)C/2h}{2+(1+m)C/4h} \simeq (1+m)\frac{C}{4h}, \quad \mathcal{T} \simeq \frac{2}{2+(1+m)C/2h} \simeq 1-(1+m)\frac{C}{4h}. \tag{125}$$

These results are formally identical to those for an abrupt change of the channel depth from h to $h-(1+m)C$.

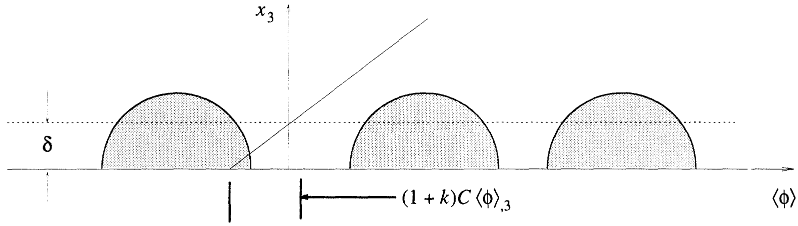

Figure 7. Interpretation of the Dirichlet results in terms of a displacement of the effective $\langle\phi\rangle = 0$ surface.

11. Summary and discussion

For the case of Dirichlet boundary conditions we have found for the ensemble-averaged field $\langle\phi\rangle$ an effective boundary condition of the form

$$\langle\phi\rangle(\boldsymbol{x}) = -(1+k)C(\boldsymbol{x})\boldsymbol{N}\cdot\nabla\langle\phi\rangle(\boldsymbol{x}), \tag{126}$$

to be applied on the smooth surface S_s supporting the roughnesses. Here C is the volume occupied by the roughnesses per unit area of the surface. In the 'dilute' limit (i.e. small fraction of area covered by the roughnesses), the dimensionless constant k only depends on the roughnesses' shape, while at finite concentrations it also depends upon their concentration.

The result (126) can readily be interpreted as follows (figure 7). For zero roughness concentration, the Dirichlet condition $\langle\phi\rangle = 0$ is satisfied on the smooth surface S_s. The presence of the roughnesses has the effect of displacing the surface where $\langle\phi\rangle = 0$ away from S_s. A linear extrapolation from this ideal surface to S_s would then give rise to the relation (126). The quantity

$$\delta = (1+k)C(\boldsymbol{x}), \tag{127}$$

which is dimensionally a length, gives a measure of the displacement of the $\langle\phi\rangle = 0$ surface from S_s. Another way to phrase our results is therefore to say that, in the presence of roughnesses, the original Dirichlet condition should be imposed on an ideal surface displaced by δ from S_s. Thus, in one of the examples of § 10, it was found that the capacitance of a rough sphere was modified as if the radius had been increased by the amount (127). From this interpretation it is also evident that, for any concentration, δ must be bounded from above by the height of the bosses.

In the case of finite concentration and hemispherical bosses, we have found (figure 6) that δ grows more slowly than linearly with C. This effect may be explained as follows. After a few bosses have been introduced, the $\langle\phi\rangle = 0$ surface, S_{eff}, say, moves a distance δ above S_s. As more bosses are added on S_s, their height above the surface S_{eff} is smaller by δ than their geometrical height. Their volume per unit area based on S_{eff} is therefore smaller than that based on S_s, and the effect of their addition thus less than proportional to C.

For the case of Neumann boundary conditions we have found

$$\boldsymbol{N}\cdot\nabla\langle\phi\rangle = \nabla_H\cdot\{C(\boldsymbol{x})[\mathcal{I}+\mathcal{M}]\cdot\nabla_H\langle\phi\rangle(\boldsymbol{x})\}, \tag{128}$$

where the subscript H indicates the gradient in the tangent plane, $\mathcal{I}$ is the identity 2×2 matrix and $\mathcal{M}$ is another 2×2 matrix dependent on the shape of the bosses. As found in two examples in § 10, here an interpretation in terms of a displacement of the 'effective' surface is still applicable provided the concentration is uniform and $\mathcal{M}$

diagonal (as is the case, e.g., for axisymmetric bosses). In the general case, however, the effect of the roughnesses is more complex.

The direct numerical simulation method used for the Dirichlet case cannot be applied to Neumann conditions. Other approaches that suggest themselves for this case are of the boundary-integral or collocation type (see, for example, Weinbaum *et al.* (1990) for a review of these approaches in the context of Stokes flow).

In deriving our results we have made a number of approximations. The first one is the separation of scales between the boss size and the local radius of curvature of the smooth surface S_s. On this basis we have approximated S_s by its tangent plane in the neighbourhood of each boss. It would appear possible to embed this procedure in a proper multiple-scales perturbation expansion of which our results would then constitute the leading-order term. Higher-order terms in this expansion, however, would probably acquire a non-local nature as implied by the regularized integral contributions in our results (see, for example, equation (37)).

Secondly, we have also assumed that any boundary other than the rough surface is sufficiently far away from each boss that the direct effect of the boss itself on this boundary is negligible. As a consequence of these two assumptions, the scale of variation of the average field $\langle\phi\rangle$ is also large with respect to the size of the bosses, which enabled us to use a linear approximation over distances comparable with the boss size. If $\langle\phi\rangle$ cannot be accurately approximated by a Taylor-series expansion, one would again find a non-local effective boundary condition as suggested by equations (33) and (34).

We have considered the dilute limit—in which the bosses only interact through the effective field—analytically and the finite-concentration case numerically. An interesting problem that remains is the analytical study of the finite-concentration case. It is likely that some form of divergence would arise, to be taken care of by a suitable renormalization procedure.

The general problem addressed in this study can be extended in several directions. For example, one may consider the inhomogeneous case (the Poisson equation) or more complicated (microscopic) boundary conditions, e.g. non-homogeneous or of the mixed (Robin) type. For the Poisson equation, if the scale of variation of the forcing is large on the scale of the bosses, it appears that the present method would go through with only slight modifications. A 'fine grain' structure of the forcing in the neighbourhood of the boundary, on the other hand, would most likely require a different approach. Since our method is built on the use of suitable Green's functions, situations in which these functions cannot be relatively simply approximated would not readily lend themselves to analysis by the present approach.

The first author is grateful to Dr A. S. Sangani for help and advice with the numerical simulation described in § 8 and to Dr H. N. Oğuz for discussions related to some of the calculations of § 7.

This study has been supported by DOE and NSF under grants DE-FG02-89ER14043 and CTS-8918144, respectively.

Appendix A.

This appendix describes the calculations leading to the evaluation of the constant k for the examples given in § 7. As a general reference we use the book by Lebedev (1965), whose notation we also adopt. As in § 8, the coordinate x_3 is taken normal to the plane.

(a) Prolate spheroid

For prolate hemispheroidal bosses, we use prolate spheroidal coordinates (ξ, η, ϕ) related to the Cartesian coordinates by

$$x_1 = d \sinh\xi \sin\eta \cos\varphi, \quad x_2 = d \sinh\xi \sin\eta \sin\varphi, \quad x_3 = d \cosh\xi \cos\eta. \tag{A 1}$$

The range of these coordinates is $0 \leqslant \xi < \infty$, $0 \leqslant \eta \leqslant \pi$ and $0 \leqslant \phi < 2\pi$. The plane corresponds to $\eta = \pi/2$, and the boss is defined by $\xi = \xi_0$, with ξ_0 given in terms of the aspect ratio Λ defined in (81) by

$$\coth\xi_0 = \Lambda \equiv b/a. \tag{A 2}$$

The constant d in (A 1) equals $a/\sinh\xi_0$.

For the Dirichlet problem, the required solution of the Laplace equation decaying at large distances from the plane is

$$X(\xi, \eta, \phi) = \sum_n T_n P_n(\cos\eta) Q_n(\cosh\xi), \tag{A 3}$$

where P_n and Q_n are the Legendre functions of the first and second kind. The boundary conditions at the wall and on the surface of the boss require that

$$T_1 = -d \frac{\cosh\xi_0}{Q_1(\cosh\xi_0)}, \tag{A 4}$$

and $T_n = 0$ for $n \neq 1$. The constant k defined by (57) is obtained from

$$k = \frac{1}{V} \int_B \frac{\partial X}{\partial \xi} x_3 \frac{h_\varphi h\eta}{h_\xi} \mathrm{d}\eta \, \mathrm{d}\varphi = -\frac{\coth\xi_0}{Q_1(\mathrm{i}\cosh\xi_0)} \left(\frac{\partial Q_1(\cosh\xi)}{\partial \xi} \right)_{\xi_0}, \tag{A 5}$$

where the h are the scale factors.

For the Neumann problem, the function M_1 is given by

$$M_1(\xi, \eta, \varphi) = \cos\varphi \sum_n U_n P_n^1(\cos\eta) Q_n^1(\cosh\xi), \tag{A 6}$$

and M_2 by a similar expression with $\cos\varphi$ replaced by $\sin\varphi$. For both M_1 and M_2 the boundary conditions require that

$$U_1 = -d \cosh\xi_0 \left(\frac{\partial Q_1^1(\cosh\xi)}{\partial \xi} \right)_{\xi_0}^{-1}, \tag{A 7}$$

while $U_n = 0$ for $n \neq 1$. Since the shape is axisymmetric, the matrix $\mathcal{M}$ is a multiple of the identity with

$$m = \frac{1}{V} \int_B M_1 n_1 h_\eta h_\varphi \, \mathrm{d}\eta \, \mathrm{d}\varphi = -\coth\xi_0 Q_1^1(\cosh\xi_0) \left(\frac{\partial Q_1^1(\cosh\xi)}{\partial \xi} \right)_{\xi_0}^{-1}. \tag{A 8}$$

(b) Oblate spheroids

For oblate spheroids, suitable coordinates are defined by (Lebedev 1965)

$$x_1 = d \cosh\xi \sin\eta \cos\varphi, \quad x_2 = d \cosh\xi \sin\eta \sin\varphi, \quad x_3 = d \sinh\xi \cos\eta. \tag{A 9}$$

The transformed coordinates have the same range as before, the plane corresponds again to $\eta = \frac{1}{2}\pi$, and the boss to $\xi = \xi_0$, with ξ_0 defined by

$$\tanh\xi_0 = \Lambda \equiv b/a. \tag{A 10}$$

In this case $d = a/\cosh\xi_0$.

The general solution appropriate for the Dirichlet problem is now

$$X(\xi,\eta,\varphi) = \sum_n T_n P_n(\cos\eta) Q_n(\mathrm{i}\sinh\xi). \tag{A 11}$$

The boundary conditions demand that the only non-vanishing coefficient be

$$T_1 = -d\frac{\sinh\xi_0}{Q_1(\mathrm{i}\sinh\xi_0)}. \tag{A 12}$$

The constant k is given by the expression

$$k = -\frac{\tanh\xi_0}{Q_1(\mathrm{i}\sinh\xi_0)}\left(\frac{\partial Q_1(\mathrm{i}\sinh\xi)}{\partial\xi}\right)_{\xi_0}. \tag{A 13}$$

For the Neumann problem, the appropriate form of the solution is

$$M_1(\xi,\eta,\varphi) = \cos\varphi U_1 P_n^1(\cos\eta) Q_n^1(\mathrm{i}\sinh\xi), \tag{A 14}$$

with M_2 obtained by changing $\cos\varphi$ to $\sin\varphi$, and

$$U_1 = -d\sinh\xi_0\left(\frac{\partial Q_1^1(\mathrm{i}\sinh\xi)}{\partial\xi}\right)_{\xi_0}^{-1}. \tag{A 15}$$

One then finds

$$m = -\tanh\xi_0 Q_1^1(\mathrm{i}\sinh\xi_0)\left(\frac{\partial Q_1^1(\mathrm{i}\sinh\xi)}{\partial\xi}\right)_{\xi_0}^{-1}. \tag{A 16}$$

(*c*) *Spherical cap*

For a spherical cap we use toroidal coordinates (ξ,η,φ) defined by (Lebedev 1965)

$$x_1 = \frac{a\sinh\xi\cos\varphi}{\cosh\xi-\cos\eta},\quad x_2 = \frac{a\sinh\xi\sin\varphi}{\cosh\xi-\cos\eta},\quad x_3 = \frac{a\sin\eta}{\cosh\xi-\cos\eta}, \tag{A 17}$$

where a is the radius of the base of the spherical segment. The plane corresponds to $\eta = 0$ and the boss to $\eta = \eta_0$ with

$$\frac{1+\cos\eta_0}{\sin\eta_0} = \Lambda. \tag{A 18}$$

For the Dirichlet problem, the appropriate solution is

$$X(\xi,\eta,\varphi) = (2\cosh\xi - 2\cos\eta)^{1/2}\int_0^\infty T(\tau)\frac{\sinh\eta\tau}{\sinh\eta_0\tau}P_{i\tau-(1/2)}(\cosh\xi)\,\mathrm{d}\tau, \tag{A 19}$$

where, from the boundary conditions (Lebedev 1965),

$$T(\tau) = -2a\tau\frac{\sinh(\pi-\eta_0)\tau}{\cosh\pi\tau}. \tag{A 20}$$

Upon substitution of (A 19) into (57), one finds (84).

For the Neumann problem we have been unable to solve the integral equation necessary to impose the boundary conditions.

Appendix B.

To set up the algebraic system of equations necessary to evaluate the constants A^{α}_{nm}, $\tilde{A}^{\alpha}_{nm}$ of § 8 *a*, the derivatives of Φ^{reg} indicated in (102) are required. We give here the results needed for the present calculations referring the reader to the paper by Sangani & Behl (1989) for details.

The periodic Green's function Ψ may be represented as

$$\Psi(\boldsymbol{r}) = \psi_1(\boldsymbol{r}) - 2\pi|x_1|/\tau, \tag{B 1}$$

where

$$\psi_1(\boldsymbol{r}) = \frac{1}{\pi h^2}\int_{-\infty}^{\infty} \mathrm{d}k \sum_{\boldsymbol{l}\neq 0} Q^{-2m}\exp(-2\pi\mathrm{i}\boldsymbol{Q}\cdot\boldsymbol{r}), \tag{B 2}$$

with

$$Q = |\boldsymbol{Q}|, \quad \boldsymbol{Q} = k\boldsymbol{e}_3 + \frac{1}{h}\left(l_1\boldsymbol{e}_1 + l_2\boldsymbol{e}_2\right). \tag{B 3}$$

Further manipulation reduces this expression to

$$\Psi = \frac{1}{\tau}(C_{\mathrm{I}} + C_{\mathrm{II}} - C^{*}_{\mathrm{III}}), \tag{B 4}$$

where

$$C_{\mathrm{I}} = \frac{\tau}{\rho^{-1/2}}\sum_{\boldsymbol{l}} \Phi_{-1/2}\left(\frac{\pi(\boldsymbol{r}-\boldsymbol{r}^{\boldsymbol{l}})^2}{\sigma}\right), \tag{B 5}$$

$$C_{\mathrm{II}} = \sigma\int_{-\infty}^{\infty} \mathrm{d}k\exp(-2\pi\mathrm{i}kx_3)\int_{1}^{\infty}\mathrm{d}\beta\sum_{\boldsymbol{l}\neq 0}\exp[-\pi\beta\sigma(q_{\boldsymbol{l}}^2+k^2) - 2\pi\mathrm{i}\boldsymbol{q}_{\boldsymbol{l}}\cdot\boldsymbol{s}], \tag{B 6}$$

$$C^{*}_{\mathrm{III}} = \sigma^{1/2}\Phi^{\text{reg}}_{-3/2}(\pi x_3^2/\sigma), \tag{B 7}$$

where

$$\boldsymbol{q}_{\boldsymbol{l}} = \frac{1}{h}\left(l_1\boldsymbol{e}_1 + l_2\boldsymbol{e}_2\right), \quad \boldsymbol{s} = x_1\boldsymbol{e}_1 + x_2\boldsymbol{e}_2. \tag{B 8}$$

Φ_m is the incomplete gamma function and the superscript 'reg' represents the regular part at $x_3 = 0$.

To calculate the derivatives appearing in (102) we need to evaluate the following derivatives:

$$\partial_3^{n-m}\Delta_m C_{\mathrm{I}} = 2\tau\rho^{-1/2}\sum_{\boldsymbol{l}}\frac{(-1)^{(3n-m)/2}(n-m)!}{((n-m)/2)!}\left(\frac{\pi}{\sigma}\right)^{(n+m)/2} \times\Phi_{(n+m-1)/2}\left(\frac{\pi(\boldsymbol{r}-\boldsymbol{r}^{\boldsymbol{l}})^2}{\sigma}\right)R_{\boldsymbol{l}}^m\cos m\theta_l, \tag{B 9}$$

$$\partial_3^{n-m}\Delta_m C_{\mathrm{II}} = \sum_{\boldsymbol{l}}{}' 2q_{\boldsymbol{l}}^m\cos m\theta_{\boldsymbol{q}_{\boldsymbol{l}}}\mathrm{e}^{-2\pi i\boldsymbol{q}_{\boldsymbol{l}}\cdot\boldsymbol{s}}(-2\pi)^{n-m}(-\pi)^m \times i^n\frac{(n-1-m)!!}{(2\pi\sigma)^{(n-m)/2}}\Phi_{-(n-m+1)/2}(\pi\sigma q_l^2), \tag{B 10}$$

$$\partial_3^n C^{*}_{\mathrm{III}} = -\sigma^{1/2}\left(\frac{-\pi}{\sigma}\right)^{n/2}\frac{n!}{(n/2)!((n-1)/2)}, \tag{B 11}$$

where R_l and θ_l are the polar representation of the projection of the vector $\boldsymbol{r}-\boldsymbol{r_l}$ on the plane $x_3=0$, and $\theta_{\boldsymbol{q}_l}$ is the polar angle of the vector $\boldsymbol{q_l}$. We further need the expressions for $\partial_3^{n-m}\tilde{\Delta}_m$ operating on C_{I} and C_{II}, which are essentially the same as above except that the cosine terms are replaced by sines. Further, the following relations are made use of:

$$\partial_3^{(n+k)-(l+m)}\Delta_l\Delta_m=\partial_3^{(n+k)-(l+m)}\Delta_{l+m}+(-m)^{-m}\partial_3^{(n+k)-(l-m)}\Delta_{l-m}, \quad l\geqslant m, \tag{B 12}$$

$$\partial_3^{(n+k)-(l+m)}\Delta_l\tilde{\Delta}_m=\begin{cases}\partial_3^{(n+k)-(l+m)}\tilde{\Delta}_{l+m}-(-m)^{-m}\partial_3^{(n+k)-(l-m)}\tilde{\Delta}_{l-m}, & l\geqslant m,\\ \partial_3^{(n+k)-(l+m)}\tilde{\Delta}_{l+m}+(-m)^{-m}\partial_3^{(n+k)-(m-l)}\tilde{\Delta}_{m-l}, & l\leqslant m.\end{cases} \tag{B 13}$$

For $\partial_3^{n+k-(l+m)}\tilde{\Delta}_l\Delta_m$, we have to switch the above expressions for $l\leqslant m$ and $l\geqslant m$. Also we have

$$\partial_3^{n+k-(l+m)}\tilde{\Delta}_l\tilde{\Delta}_m=-\partial_3^{(n+k)-(l+m)}\Delta_{l+m}+(-m)^{-m}\partial_3^{(n+k)-(l-m)}\Delta_{l-m}, \quad l\geqslant m. \tag{B 14}$$

The above expressions for the derivatives are following the second method in Sangani & Behl (1989). The constant σ is arbitrary and arises from the application of Ewald's theta transform (Hasimoto 1959). It provides a convenient way of checking the numerical program by demanding invariance of the results upon changing σ. To find the regular part of the derivatives of $\Phi(\boldsymbol{r}^\alpha)$ in equation (102), we recognize that the derivatives of the regular part are regular while the derivatives of the singular part are singular. The singular part of Ψ is contained in C_{I} when this quantity is evaluated at zero and is the monopole term ($\sim 1/r$) corresponding to that boss. It can be easily subtracted out of the gamma function.

To calculate the far-field effect of having the bosses on the plane we need the limit of of $\Psi(\boldsymbol{r})$ as $x_3\to\infty$ and we recognize that the terms involving ψ_1 will not contribute in this limit. The other term in equation (B 1), however, gives a non-zero contribution since

$$\partial_3|x_3|=H(x_3)-H(-x_3), \tag{B 15}$$

where H is the Heaviside function. Noting also that $\Delta_0=2$, we obtain from (90)

$$\Phi(\boldsymbol{r})\to x_3-\frac{4\pi}{h^2}\sum_{\alpha=1}^{N_B}A_{10}^\alpha. \tag{B 16}$$

References

Batchelor, G. K. 1972 Sedimentation in a dilute dispersion of spheres. *J. Fluid Mech.* **52**, 245–268.

Beavers, G. S. & Joseph, D. D. 1967 Boundary conditions at a naturally permeable wall. *J. Fluid Mech.* **30**, 197–207.

Biot, M. A. 1968 Generalized boundary conditions for multiple scatter in acoustic reflection. *J. Acoust. Soc. Am.* **44**, 1616–1622.

Miksis, M. J. & Davis, S. H. 1994 Slip over rough and coated surfaces. *J. Fluid Mech.* **273**, 125–139.

Foldy, L. L. 1945 The multiple scattering of waves, I. General theory of isotropic scattering by randomly distributed scatterers. *Phys. Rev.* **67**, 107–119.

Hasimoto, H. 1959 On the periodic fundamental solutions of the Stokes equations and their application to viscous flow past a cubic array of spheres. *J. Fluid Mech.* **5**, 317–328.

Ishii, K. 1979 Viscous flow past multiple planar arrays of small spheres. *J. Phys. Soc. Japan.* **46**, 675–680.

Jansons, K. M. 1988 Determination of the macroscopic (partial) slip boundary condition for a viscous flow over a randomly rough surface with a perfect slip microscopic boundary condition. *Phys. Fluids* **31**, 15–17.

Kress, R. 1989 *Linear integral equations*, vol. 82, *Applied Mathematical Science*, Berlin: Springer.

Lebedev, N. N. 1965 *Special functions and their applications.* Englewood Cliffs, NJ: Prentice Hall (reprinted 1972 Dover: New York).

Lucas, R. J. & Twersky, V. 1988 High-frequency reflection and scattering of sound by ellipsoidally embossed surfaces. *J. Acoust. Soc. Am.* **83**, 2005–2011.

Nield, D. A. 1983 The boundary condition for the Rayleigh-Darcy problem: limitations of the Brinkman equation. *J. Fluid Mech.* **128**, 37–46.

Ogilvy, J. A. 1987 Wave scattering from rough surfaces. *Rep. Prog. Phys.* **50**, 1553–1608.

Ogilvy, J. A. 1991 *Theory of wave scattering from random rough surfaces.* Bristol: Hilger.

Richardson, S. 1971 A model for the boundary condition of a porous material. Part 2. *J. Fluid Mech.* **49**, 327–336.

Rosales, R. R. & Papanicolaou, G. C. 1983 Gravity waves in a channel with a rough bottom. *Stud. Appl. Math.* **68**, 89–102.

Saffman, P. G. 1971 On the boundary condition at the surface of a porous medium. *Stud. Appl. Math.* **1**, 93–101.

Sangani, A. & Behl, S. 1989 The singular solution of Stokes and Laplace equations and their application to transport processes near porous surfaces. *Phys. Fluids* A **1**, 21–37.

Sarkar, K. 1994 Effective boundary conditions for rough surfaces and acoustics of oceanic bubbles. Doctoral dissertation, Department of Mechanical Engineering, The Johns Hopkins University.

Sarkar, K. & Prosperetti, A. 1996 Effective boundary conditions for Stokes flow over a rough surface. *J. Fluid Mech.* (submitted).

Stakgold, I. 1979 *Green's functions and boundary-value problems.* New York: Wiley.

Taylor, G. I. 1971 A model for the boundary condition of a porous material. Part 1. *J. Fluid Mech.* **49**, 319–326.

Tolstoy, I. 1980 Coherent acoustic scatter at a rough interface between two fluids. *J. Acoust. Soc. Am.* **66**, 258–268.

Tolstoy, I. 1984 Smoothed boundary conditions, coherent low-frequency scatter, and boundary modes. *J. Acoust. Soc. Am.* **75**, 1–22.

Tolstoy, I. 1986 Long-wavelength acoustical scatter from rough surfaces. In *Frontiers in physical acoustics, Proc. Int. School of Physics 'Enrico Fermi'* (ed. D. Sette), pp. 209–254. Amsterdam: North-Holland.

Twersky, V. 1951 On the nonspecular reflection of sound from planes with absorbent bosses. *J. Acoust. Soc. Am.* **23**, 336–338.

Twersky, V. 1957 On scattering and reflection of sound by rough surfaces. *J. Acoust. Soc. Am.* **29**, 209–225.

Twersky, V. 1983 Reflection and scattering of sound by correlated rough surfaces. *J. Acoust. Soc. Am.* **73**, 85–94.

Weinbaum, S., Ganatos, P. & Yan, Z. Y. 1990 Numerical multipole and boundary integral equation techniques in Stokes flow. *A. Rev. Fluid Mech.* **22**, 275–316.

Received 25 April 1994; accepted 16 January 1995